www.czasopisma.pan.pl PAN www.journals.pan.pl

ARCHIVES of FOUNDRY ENGINEERING

VERSITA

DOI: 10.2478/afe-2013-0074

ISSN (2299-2944)
Volume 13
Issue 4/2013

9 – 14

Published quarterly as the organ of the Foundry Commission of the Polish Academy of Sciences

Cellular Automaton Modeling of Ductile Iron Density Changes at the Solidification Time

A.A. Burbelko[a]*, D. Gurgul[a], M. Królikowski[a,b], M. Wróbel[a]

[a] Faculty of Foundry Engineering, AGH University of Science and Technology, Reymonta Str. 23, 30-059 Krakow, Poland

[b] Odlewnie Polskie S.A., Wyzwolenia Ave. 70, 27-200 Starachowice, Poland

* Corresponding author. E-mail address: abur@agh.edu.pl

Received 28.06.2013; accepted in revised form 02.09.2013

Abstract

Formation of the shrinkage defects in ductile iron castings is far more complicated phenomenon than in other casting alloys. In the paper one of the aspects of formation of porosity in this alloy was considered – changes in cast iron's density during crystallization caused by varying temperature, phase fractions and phase's composition. Computer model, using cellular automata method, for determination of changes in density of ductile iron during crystallization was applied. Simulation of solidification was conducted for 5 Fe-C binarie alloys with ES from 0.9 to 1.1 for the estimation of the eutectic saturation influence on the ductile iron shrinkage and expansion. As a result of calculations it was stated that after undercooling ductile iron below liquidus temperature volumetric changes proceed in three stages: pre-eutectic shrinkage (minimal in eutectic cast iron), eutectic expansion (maximum value equals to about 1.5% for ES = 1.05) and last shrinkage (about 0.4% in all alloys regardless of ES).

Keywords: Cellular Automaton, Ductile Iron, Pre-eutectic Shrinkage, Eutectic Expansion

1. Introduction

Density of the majority of known substances is increased during transition from liquid to solid state. It means that volume of the solid is smaller compared to volume of the liquid it solidified from. Exceptions from this behaviour exhibits e.g. water or bismuth. Volume of this substances increases during crystallization due to specific structure of crystal lattice. In foundry engineering it causes the need of feeding solidifying castings in order to eliminate shrinkage defects.

Similarly to water and bismuth cast iron with high carbon concentration behaves. The reason for this increase in the volume during crystallization is participating of graphite, which density is almost three times smaller than other phases. Still, practical foundry knowledge shows that obtaining "healthy" casting, meaning without shrinkage defects, made of ductile iron (DI) is very difficult for small values of casting's thermal module (under about 12 mm) [1].

It is known that expansion of DI is few times greater than cast iron with flake graphite [2]. As a result of increase in volume caused by participating of graphite in initial stage of crystallization the metallostatic pressure may rise [3]. If the casting mould isn't rigid enough it may lead to irreversible deformation of its walls (swelling of the mould) [4]. An increase in volume of mould cavity due to swelling is considered one of the reasons for forming of the shrinkage defects in DI castings solidifying in "vulnerable" moulds.

Conditions of graphite growth in DI differs considerably from other grades of cast iron. In grey cast iron both primary and eutectic graphite are in constant contact with dwindling liquid phase. Additionally, eutectic graphite – during crystallization – grows in conditions of constant contact of three phases.

In DI globules of primary and eutectic graphite in initial stage of crystallization don't have touch with austenite grains and grow directly from the liquid [5, 6]. In a time a contact between grains of those phases is formed. A layer of austenite quickly isolates graphite form the liquid. Later on the graphite only grows by diffusion of carbon from liquid through the austenite shell.

Probably that's the reason for shrinkage phenomena in DI castings to be more complicated than in other casting alloys.

Castings made of DI in Odlewnie Polskie S.A. are characterized by the same, known from literature, shrinkage defects typical for this alloy [4]:

1) the mechanism of feeders performance is far more complicated than in alloys which has no expansion; sometimes by elimination of the feeders causes decrease in porosity;
2) minimal porosity occurs in eutectic alloys, wherein an increase in carbon concentration in eutectic (having conserved ES = 1.0) has positive effect;
3) porosity of grey iron castings is considerably smaller than that of DI.

Examples of dispersed and concentrated shrinkage porosity that may occur in industrial castings made of DI are shown in fig. 1. Such defects have negative effect on strength and leakproofness of castings.

The mechanisms of shrinkage defects formation are still being discussed, though it is obvious that major reason for that is change in volume of an alloy during cooling and phase transitions. This paper presents assessments of change in specific volume of DI during crystallization using cellular automata method.

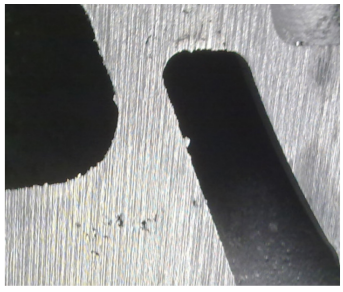

a)

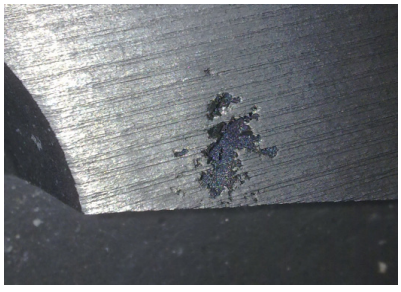

b)

Fig. 1. Examples of shrinkage defects in DI castings: a) dispersed porosity; b) concentrated porosity

Examples of shrinkage cavity shape in industrial casting's feeders made of DI EN-GJS-400-18 with differing carbon concentration are shown in fig. 2. Carbon concentration was evaluated using value of Active Carbon Equivalent measured by Adaptive Thermal Analysis System (ATAS). Value of ACEL is changed from 4.15 to 4.28%. Fig. 2 shows that with an increase in carbon concentration the volume of voids in the feeder decreases. Unfortunately, experience dictates that it doesn't always lead to reduction of shrinkage defects level in casting itself.

2. Model of process

2.1. Cellular automata in the solidification modeling

The Cellular Automata - Finite Differences method (CA-FD) is one of the known methods of the simulation of microstructure formation during solidification. In the CA microstructure modeling the grain shape during and after solidification is the result of the simulation and does not superimposed beforehand. The model development for a one-phase microstructure evolution is a subject of the numerous researches [7-16]. Known models of the eutectic solidification of DI are not so numerous [6, 17-22].

Model used in this paper is based on the CA-FD technique and will predict solidification of DI during the cooling of the casting region with the superimposed cooling rate. Model takes into account the continuous nucleation of austenite and graphite grains from liquid controlled by undercooling, separate non-equilibrium growth of graphite nodules and austenite dendrites at the first solidification stage, and the following cooperative growth of graphite-austenite eutectic in the binary Fe-C system. Detailed description of the model was presented in [6, 20-22].

2.2. Density estimation

Density of specific phases was determined using Thermo-Calc software. For graphite calculations were performed with the temperature range of 1010 to 1610 K with 10 K step. For austenite the temperature range was 1010 to 1610 K with 100 K step and carbon concentration in solution ranging from 0.5 to 2.5 mass % with 0.05% step. For liquid phase density was calculated for the same temperature range as in austenite but for carbon concentration from 3.9 to 4.8 mass% with 0.0225% step. Using obtained data regression equations were determined by the least squares method. Those equations were implemented into computer model to calculate densities of each phase (kg/m^3):

- graphite density:

$$\rho_{gr} = 2292.9 - 0.067442T \quad (1)$$

- austenite density:

$$\rho_{\gamma} = 8238.7 - 0.48684T - 3876.C - 5982.0C^2 \quad (2)$$

- liquid density:

$$\rho_L = 8192.2 - 0.5402T - 9805.3C \quad (3)$$

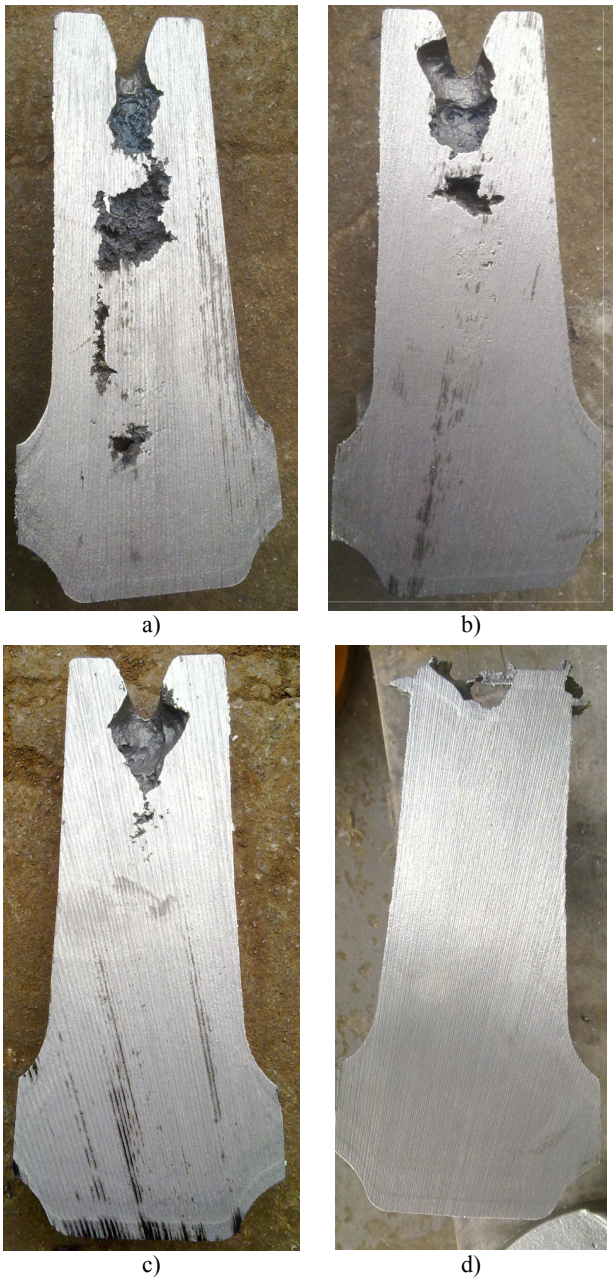

a) b) c) d)

Fig. 2. Influence of the Active Carbon Equivalent on the pipe shape in the feeder of EN-GJS-400-15 casting; ACEL values: a) 4.15%, b) 4.18%, c) 4.22%, d) 4.28%

In above equations temperature is in absolute scale (K) and carbon concentration is in mass fraction. The mean value of the alloy density at the steps of the solidification path was calculated as a weighted mean value of the phases' density. As a weight coefficients the phase volume fractions were used.

3. Results of investigations

Carbon concentration in cast iron has substantial influence on shrinkage phenomena, because it determines amount of graphite in the microstructure. It is known that nature of this dependence is extremal. Experience shows that minimal level of shrinkage defects occurs in cast iron with eutectic carbon concentration. It is considered that in hypoeutectic cast iron carbon concentration isn't high enough for expansion – dependent on amount of crystallized graphite – to compensate shrinkage. On the other hand it was supposed that in hypereutectic cast iron crystallization of primary graphite, directly from the liquid phase, leads to excessive expansion still before beginning of crystallization of eutectic.

This paper presents results of forecasting the change in density of binary Fe-C alloy during crystallization for five values of the eutectic saturations (0.90, 0.95, 1.00, 1.05 and 1.10).

Computations were carried out on a 2D grid of 640×640 cells. The side of each cell was 1 μm in length. An initial uniform carbon concentration in the binary Fe-C liquid was assumed. Modelling was carried out for cooling of the specimen with constant heat removal, which without phase transitions causes cooling rate to be equal to 10 K/s.

Results of the temperature change simulations of specimens are shown in fig. 3 along with changes of the cast iron's specific volume. Presented data concerns period starting with passing the liquidus temperature down to instant of crystallization termination. It means that shrinkage of the liquid phase above liquidus and shrinkage of solid phases after completion of crystallization isn't taken into account in this simulation. Change in specific volumes of alloys vs. solid fraction are shown in fig. 4.

The reason for lack of recalescence on the cooling curves of hypoeutectic cast iron in figs. 3a-b may be use of constant cooling rate in simulation.

Fig. 3 shows that for each of analysed alloys change on volume may be divided into three stages:

- pre-eutectic shrinkage;
- eutectic expansion;
- final shrinkage.

The magnitude of volume change of each stage for cast iron with different eutectic saturations is shown in fig. 5.

Pre-eutectic shrinkage occurs not only in hipo- or hypereutectic cast iron. In eutectic alloy though its intensity and duration are minimal. As a result of pre-eutectic shrinkage specific volume of the eutectic cast iron diminishes only by 0.3% vol. compared to specific volume at liquidus temperature (fig. 5). In the case of hypereutectic cast iron it means that participating of nodular, primary graphite in the first stage of crystallization does not compensate shrinkage. An increase in liquid's density due to both decrease of temperature and carbon concentration – see Eq. (3) – is stronger at this stage than decrease of density as a result of crystallization of graphite globules.

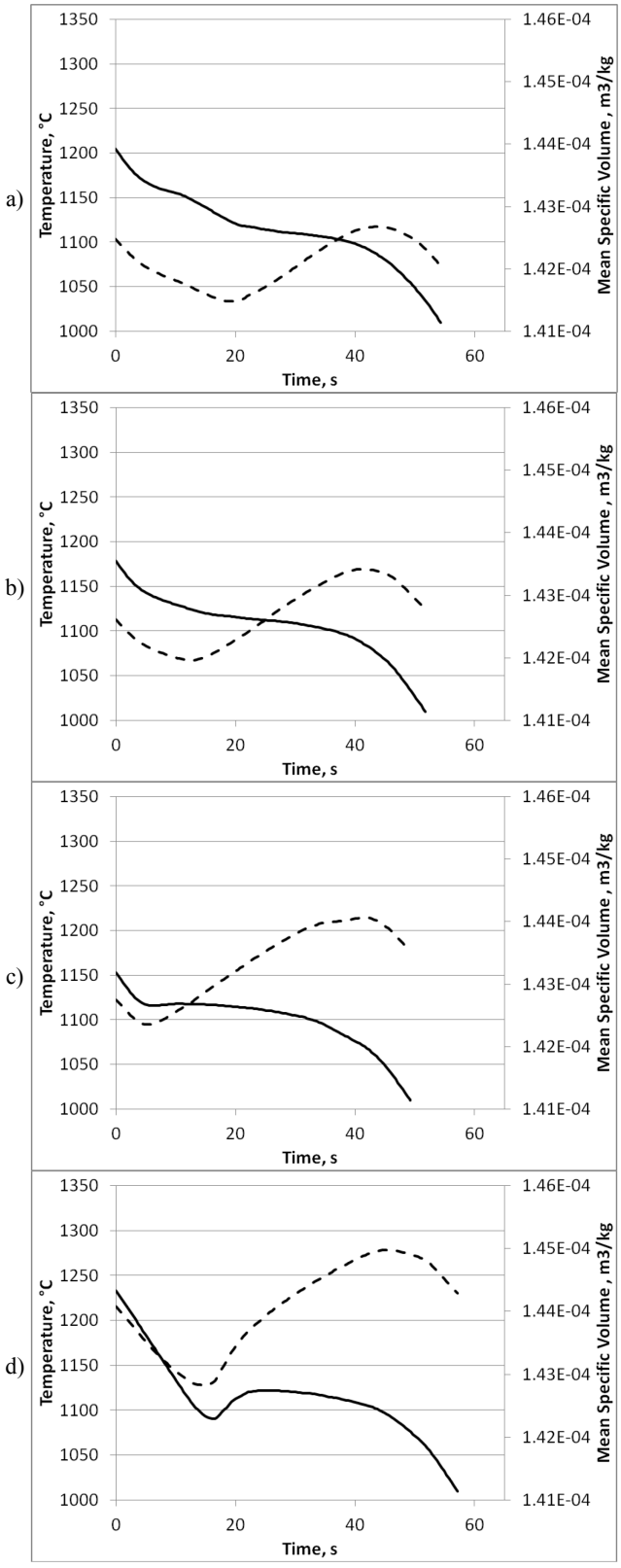

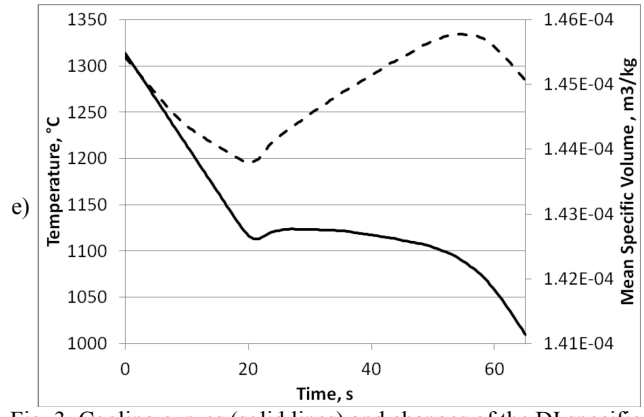

Fig. 3. Cooling curves (solid lines) and changes of the DI specific volume (dashed lines) during the solidification for the eutectic saturation, ES: a) 0.90, b) 0.95, c) 1.00, d) 1.05, e) 1.10

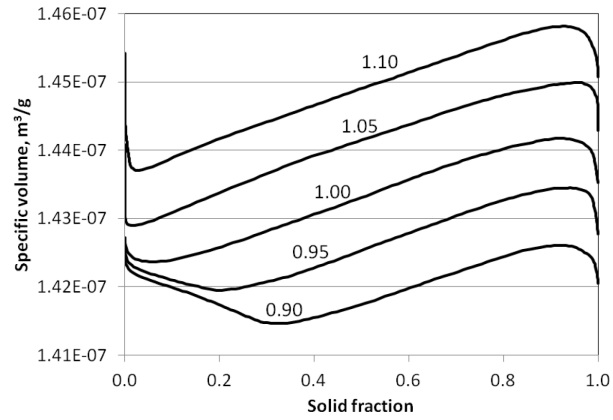

Fig. 4. Changes of the DI specific volume as a solid fraction function for different levels of the eutectic saturation, ES

Magnitude of last shrinkage practically does not depend on carbon concentration (fig. 6).

Similar mechanism can be observed at the beginning of crystallization of eutectic cast iron, because at the beginning graphite globules in eutectic and hypoeutectic cast iron nucleates and grow (same as primary graphite in hipereutectic cast iron) without connection to austenite dendrites. It is shown on maps obtained during formation of DI structure (fig. 5).

Expansion of eutectic (fig. 3c) and hipereutectic (fig. 3d, e) cast iron begins simultaneously with commencement of recalescence.

a)

b)

c)

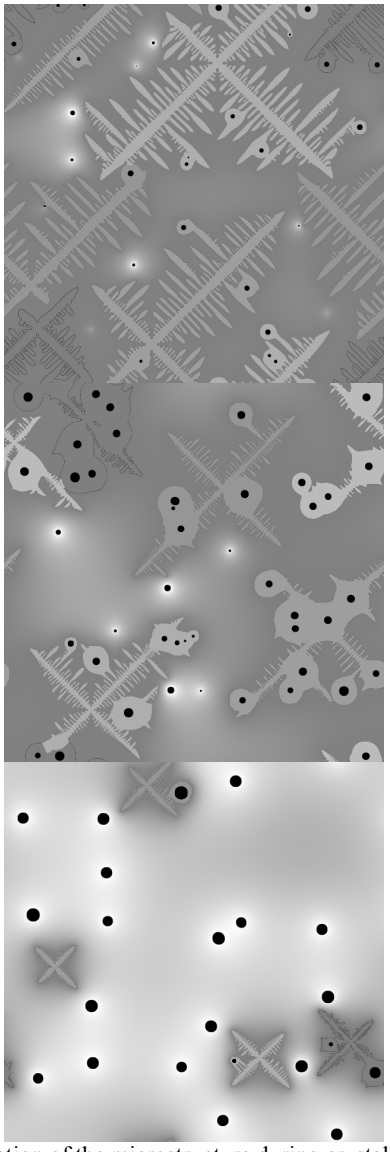

Fig. 5. Formation of the microstructure during crystallization of DI for composition: a) hypereutectic - ES = 0.90, b) eutectic – ES = 1.00, c) hipereutectic - ES = 1.10

4. Conclusions

The CAFD computer model was used for the prediction of the DI density changes in the solidification time. Results of modelling allow to better understand nature and mechanism of formation of shrinkage defects in this casting material.

It was shown that for all analysed compositions (with Eutectic Saturation from 0.90 to 1.10) the course of the volumetric changes during the solidification consist from tree phases: pre-eutectic shrinkage, eutectic expansion and last shrinkage.

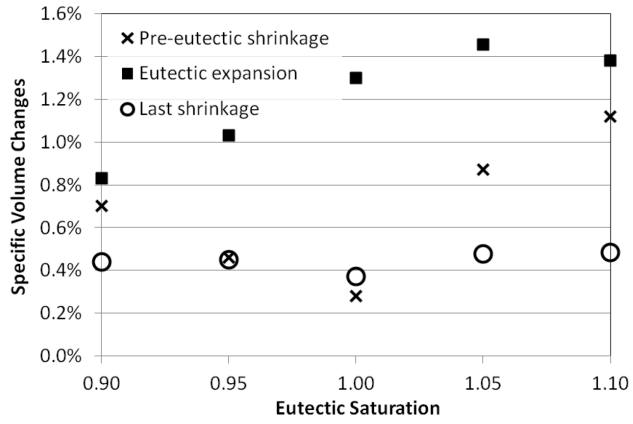

Fig. 6. Components of the volumetric change of the DI with different levels of the eutectic saturation during the solidification

Among analysed alloys minimal level of the pre-eutectic shrinkage is observed in eutectic cast iron. Maximal level of the eutectic expansion however occurs in the alloy with ES = 1.05.

Acknowledgements

This work was supported by Polish National Science Centre (project No. DEC-2011/01/B/ST8/01689)

References

[1] The Sorelmetal Book of Ductile Iron. (2004). Rio Tinto iron & titanium, p. 174.

[2] Nandori, G., (1996). Relation between the volume change during the solidification of lamellar and ductile cast iron and the crystallization sequence, *Materials Science Forum*, *Vol. 215-216,* pp. 399-407.

[3] Gedeonova, Z., (1996). et al.: Displacement of the Surface Mould and Metal during the Solidification of Nodular Graphiet Iron Casting, *Materials Science Forum*, *Vols. 215-216,* pp. 391-398.

[4] Ohnaka, I., Sato, A., Sugiyama, A., & Kinoshita F. (2008). Mechanism and estimation of porosity defects in ductile cast iron, International *Journal of Cast Metals Research*, *Vol. 21, no 1-4,* p. 11-16.

[5] Fredriksson, H., Stjerndahl, J., & Tinoco, J. (2005). On the solidification of nodular cast iron and its relation to the expansion and contraction, *Materials Science and Engineering A, Vol. 413–414,* pp. 363–372.

[6] Burbelko, A., Fraś, E., Gurgul, D., Kapturkiewicz, W., & Sikora, J. (2011). Simulation of the ductile iron solidification using a cellular automaton, *Key Engineering Materials, Vol. 457,* pp. 330-336.

[7] Umantsev, A.R., Vinogradov, V.V. & Borisov, V.T. (1985). Mathematical modeling of the dendrite growth during the solidification from undercooled melt, *Kristallografia*, *Vol. 30,* pp. 455-460 (in Russian).

[8] Rappaz, M., & Gandin, Ch.A. (1993). Probabilistic Modelling of Microstructure Formation in Solidification Processes, *Acta Metallurgica et Materialia*, *Vol. 41,* p. 345-360.
[9] Pan, S. & Zhu, M. (2010). A three-dimensional sharp interface model for the quantitative simulation of solutal dendritic growth, *Acta Materialia, Vol. 58.* p. 340-352.
[10] Guillemot, G., Gandin, Ch.A. & Bellet, M. (2007). Interaction between single grain solidification and macrosegregation: Application of a cellular automaton-finite element model, *Journal of Crystal Growth*, *Vol. 303.* p. 58-68.
[11] Beltran-Sanchez, L. & Stefanescu, D.M. (2004). A quantitative dendrite growth model and analysis of stability concepts, *Metall. Mat. Trans. A, Vol. 35,* p. 2471-2485.
[12] Pavlyk, V. & Dilthey, U. (2004). Simulation of weld solidification microstructure and its coupling to the macroscopic heat and fluid flow modelling, *Modelling and Simulation in Materials Science and Engineering*, *Vol. 12*, p. 33-45.
[13] Zhu, M.F., & Hong, C.P. (2002). A three dimensional modified cellular automaton model for the prediction of solidification microstructures, *ISIJ International*, *Vol. 42,* p. 520-526.
[14] Jarvis, D.J., Brown, S.G.R. & Spittle J.A. (2000). Modelling of non-equilibrium solidification in ternary alloys: comparison of 1D, 2D, and 3D cellular automaton-finite difference simulations, *Mat. Sci. Techn., Vol. 16 p.* 1420-1424.
[15] Burbelko, A.A., Fraś, E., Kapturkiewicz, W., & Gurgul, D. (2010). Modelling of dendritic growth during unidirectional solidification by the method of cellular automata, *Mat. Sci. Forum*, *Vol. 649,* p. 217-222.
[16] Burbelko, A.A., Fraś, E., Kapturkiewicz, W. & Olejnik, E. (2006). Nonequilibrium kinetics of phase boundary movement in cellular automaton modelling, *Mat. Sci. Forum*, *Vol. 508,* p. 405-410.
[17] Zhu, M., Pan, S., Sun, D., & Zhao, H. (2010). Numerical Simulation of Microstructure Evolution During Alloy Solidification by Using Cellular Automaton Method, *SIJ International*, *Vol. 50, No. 12,* pp. 1851–1858.
[18] Zhao, H.L., Zhu, M.F. & Stefanescu, D.M.: (2011). Modeling of the divorced eutectic solidification of spheroidal graphite cast iron, *Key Eng. Materials*, *Vol. 457,* pp. 324-329.
[19] Kapturkiewicz, W., Burbelko, A.A., Fraś, E., Górny, M. & Gurgul, D. (2010). Computer modelling of ductile iron solidification using FDM and CA methods, Journal of *Achievements in Materials and Manufacturing Engineering*, *Vol. 43,* pp. 310-323.
[20] Burbelko, A.A., Gurgul, D., Kapturkiewicz, W. et al.: Cellular automaton modelling of ductile iron microstructure in the thin wall casting, *IOP Conference Series-Materials Science and Engineering*, *Vol. 33, Art. Nr: 012083.*
[21] Gurgul, D., Burbelko, A.A., Fraś, E. & Guzik E. (2010). Multiphysics and multiscale modelling of ductile cast iron solidification. *Archives of Foundry Engineering. Vol. 10,* pp. 35-40.
[22] Gurgul D. & Burbelko A. (2010). Simulation of Austenite and Graphite Growth in Ductile Iron by means of Cellular Automata, *Archives of Metallurgy and Materials*, *Vol. 55,* pp. 53-60.